Airgap Search Coil-based Detection of Damper Bar Failures in Salient Pole Synchronous Motors

J. Yun[*,**], S. Park[**], C. Yang[**], S.B. Lee[**], J. Antonino-Daviu[***], M. Sasic[****] and G.C. Stone[****]

[*]Hyundai Electric, Yongin, Korea

[**]Korea University, Seoul, Korea

[***]Universitat Politecnica de Valencia, Valencia, Spain

[* ***]Qualitrol-Iris Power Engineering, Mississauga, ON, Canada

***Abstract*—Damper bars are often used in high output salient pole synchronous motor (SM) rotors for motor starting and stabilization of performance. Several cases of broken damper bars in the rotor of SMs that lead to motor starting failure and/or forced outage have recently been reported. However, detection of damper bar failures is difficult, since the damper bars are active only under the starting or load transients. Damper bar testing in the field currently relies on off-line visual inspection, and there is no means available for detecting failures on-line. In this paper, a new method for detecting damper bar failures based on the analysis of airgap search coil measurements under the starting transient is proposed. Since airgap search coils are being increasingly installed in large SMs for detecting field winding short circuits, the proposed method can be implemented without additional hardware. The effectiveness of the proposed method is verified with 2 dimensional finite element analysis and experimental testing on a custom-built 30 kW salient pole SM under controlled fault conditions. It is shown that the proposed method can provide reliable and sensitive detection of broken damper bars whenever the motor is started at low additional cost.**

***Index Terms*—Airgap Flux, Fault Diagnostics, Salient Pole Synchronous Motor, Search Coil, Spectral Analysis, Starting Transient.**

I. Introduction

Although synchronous motors (SMs) provide constant speed operation at high power factor and efficiency with low inrush current, they are limited to high output motors (> 5 MW) due to their relatively high cost over induction motors. The reliability is critical for most large SM applications, and condition monitoring that can provide advanced warning to any of the faults developing in the motor is vital for continued operation of the industrial facility [1]-[6]. The damper bars (or amortisseur windings) in the rotor of direct on-line started SMs is an important component that enables starting of the motor. It also improves the operating stability and motor performance under non-ideal supply conditions and load transients. Although damper bar failures are not as common as stator or field winding insulation or bearing failures, damage in the damper bar or short circuiting segments have recently been reported, as shown in Fig. 1. An open circuit in the damper bars of high output salient pole synchronous machines used in compressor, pumped storage generation, and synchronous condenser applications have been reported to cause performance degradation, starting failure, or forced outage of the motor or industrial process that they drive [2]-[7].

Damper bar breakage can occur due to deficient design or construction of the motor [8]-[9], or mis-operation [4], but is mainly caused by the thermo-mechanical stress due to uneven thermal expansion during the starting transient. The current distribution in the damper bars is uneven for salient pole rotors where the current in the bars in the pole edges are the largest [3], [10], [11]. This produces mechanical stress on the damper bars since the temperature rise and degree of axial thermal expansion is uneven between the bars. The brazed portion in pole edge bars are most vulnerable to damage, and failures are most common in applications frequent starts or large load variations [4]-[5]. Broken damper bars exert more stress on the remaining bars leading to additional breakages, and slows down motor acceleration until it is unable to start [2].

Despite the serious consequences of damper bar failure, testing in the field currently relies on off-line visual inspection, where one searches for signs of discoloration or cracks visually or with a borescope [3]-[4]. Damper bar failures are difficult to detect since current is induced only during starting or load transients. There has not been much research activity on damper bar fault detection other than some rudimentary methods. In [2]-[3], detection of damper bars based on the acceleration time, current or airgap flux amplitude during the starting transient have been studied; however, they lack sensitivity and reliability as they could be influenced by supply, motor, or load conditions. In [12], monitoring of the rotor rotational frequency sideband component in the stator current in steady state is proposed as an indicator of broken damper bars. However, this component is known to be produced by any type of rotating asymmetry in a machine [13], and the method relies on non-ideal supply frequency components induced in the damper bars in steady state. In [9], monitoring of the twice slip frequency rotor cage fault sideband components during the starting transient was proposed for cylindrical rotor SMs. This method cannot be applied to

(a) (b)

Fig. 1 Damper bar failure in 11 kV, 33 MW, 26 pole salient pole synchronous motor; (a) pole surface; (b) broken damper bar

motors with salient pole rotors since the saliency produces frequency components that are identical to that of broken damper bars [6]. An extensive literature survey shows that there is currently no means of detecting broken damper bars for salient pole SMs when the motor is operating. In [2], [5]-[7], leading SM manufacturers confirm that damper winding failures is a serious issue and that there is no known on-line detection method available for salient pole SMs.

Considering the serious consequences of damper bar failure and lack of test method in the field for dampers, detection of broken damper bars in salient pole SMs is needed. In this paper, a new method that monitors the damper bar condition during the motor starting transient based on the airgap search coil measurement available in the SM is presented as a viable solution. A finite element study and experimental test results on a custom built 30 kW salient pole SM under controlled fault conditions are provided to show that the proposed method is capable of sensitive and reliable detection of damper bar failures during motor starting.

II. Flux Based Detection of Broken Damper Bars During Motor Starting

Airgap search coils have been used since the 1970s for detecting interturn short circuits in the field winding of synchronous generators and motors [1], [14]. Field winding short circuits are mainly caused by degradation of turn insulation due to the mechanical and thermal aging. Since shorted turns in the field winding can produce excessive vibration that degrades performance and reliability, many off-line and on-line test methods for shorted field winding have been developed over the years. It has been shown that airgap flux-based fault monitoring is the most effective means of detecting the failure for both cylindrical and salient pole machines [1], [15]-[16]. Airgap search coils as thin as 4 mm have become commercially available and are being increasingly installed on the stator tooth surface of SMs for detecting interturn shorts in the field winding, as shown in Fig. 2. The main idea of the proposed method is to take advantage of the airgap flux sensor in the motor, and analyze the measurement obtained during the motor starting transient to detect broken damper bars in salient pole SMs.

When a SM is line-started with a 3 phase sinusoidal supply, the field winding is de-energized and short circuited through a starting resistor to prevent induction of high voltage across the field winding. The typical range of the value of the starting resistor is between 6 to 20 times the dc field winding resistance. The current induced in the damper winding produces the torque that starts and accelerates the rotor as in the case of induction motors. The dc field voltage is applied after the rotor reaches 95% of rated speed to pull the rotor into synchronization [17]. Once the rotor reaches steady state, the field winding produces the synchronous torque, and the damper winding becomes inactive, where only small amplitude current components are induced by harmonics. Since the damper bar current and airgap flux are the highest in amplitude during the starting transient, as shown in Fig. 3, detection of damper winding faults is expected to be most sensitive at that time.

The airgap search coil voltage signal during the starting transient includes multiple frequency components as shown in Fig. 3 (for a 4 pole salient pole SM). The main component is the input supply frequency, f_s, since the stator current and induced damper bar current are always at f_s when viewed from the fixed flux coil in the stationary reference frame. For salient pole motors, there is large fluctuation in the airgap flux due to the variation in magnetic reluctance as a function of rotor position. Therefore, integer multiples, k, of the once per revolution (or 1X) rotor rotational frequency component, f_r, given by

$$f_r = (1 - s) \cdot f_s / p \tag{1}$$

have a significant influence on the flux coil measurements where p is the number of pole pairs and s is the rotor slip. The supply frequency signal is modulated by the integer multiples of f_r, and this induces k-f_r sidebands of f_s, f_{flux}, in the flux coil voltage, which can be used for detecting damper bar failure.

$$f_{flux} = f_s \pm k \cdot f_r = (1 + k \cdot (1 - s)/p) \cdot f_s, \tag{2}$$

The influence of the salient poles, and the higher frequency components produced by the damper bar slots can be observed in the flux waveform during the starting transient in the zoomed-in part Fig. 3. The f_r and f_{flux} components vary as the rotor accelerates from standstill to synchronous speed since s decreases from 1 to 0. The change in the f_{flux} components during the starting transient for s=1, 0.5, and 0 are summarized

Fig. 2 Commercial airgap search coil installed on stator tooth surface for detecting short circuits in field winding of synchronous machine [17]

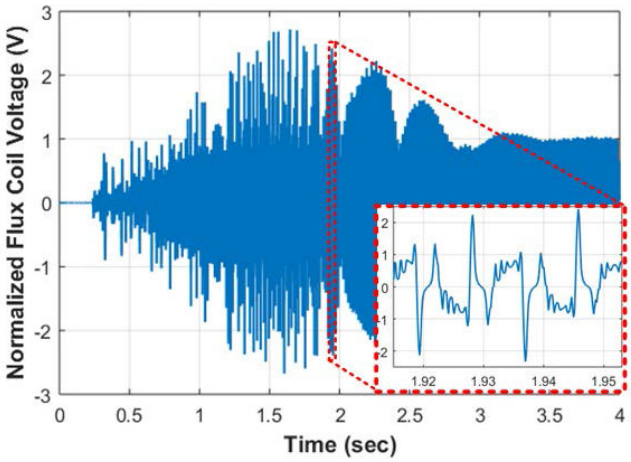

Fig. 3 Airgap search coil voltage measurement during motor starting for 4 pole salient pole SM

Table I. Variation in f_{flux} components in the flux for 4 pole motors for different values of k (up to ±12) as the rotor accelerates from standstill to synchronous speed ($s: 1 \rightarrow 0$)

k	0	+1	+2	+3	+4	+5	+6	+7	+8	+9	+10	+11	+12
s=1	60	60	60	60	60	60	60	60	60	60	60	60	60
s=0.5	60	75	90	105	120	135	150	165	180	195	210	225	240
s=0	60	90	120	150	180	210	240	270	300	330	360	390	420
k	0	-1	-2	-3	-4	-5	-6	-7	-8	-9	-10	-11	-12
s=1	60	60	60	60	60	60	60	60	60	60	60	60	60
s=0.5	60	45	30	15	0	-15	-30	-45	-60	-75	-90	-105	-120
s=0	60	30	0	-30	-60	-90	-120	-150	-180	-210	-240	-270	-300

in Table I for different values of k up to ±12 for a 4 pole motor. It can be seen that the variation of the f_{flux} pattern is different for each k value. Since there are multiple components that change in amplitude and frequency as the motor accelerates, it is difficult to identify the components in the time domain.

The main sideband components in the airgap search coil measurement depends on the number of poles since the flux amplitude changes every time the salient pole of the rotor passes the search coil. Since the search coil "sees" $2p$ poles per rotor rotation, frequency components will be induced at integer multiples of k=±$2p$ in the flux signal due to saliency. For a 4 pole motor (p=2), the flux signal will include components for k=±4, ±8, ±12,… in addition to f_s. When a broken damper bar is present in one of the poles, this produces asymmetry in the rotor that is seen once per rotor revolution by the search coil. This induces frequency components at integer multiples of k=±1 in the flux signal. Broken damper bars can therefore be detected by monitoring the multiples of k=±1 in f_{flux} in the search coil signal that are not multiples of k=±$2p$ during the starting transient. The damper bar induced components are not observable once the motor reaches steady state since there is no current in the damper bars.

III. Time Frequency Analysis of Search Coil Signal

A. Time-Frequency Representation

Since the search coil signal is non-stationary during the starting transient as shown in Fig. 3, the conventional Fourier transform cannot be applied for analysis of frequency content. A suitable time-frequency analysis technique is required to observe how the frequency contents change over time during motor starting transient. In this work, the short time Fourier transform (STFT) is used to process the signals, since it was shown to provide sufficient clarity in detecting motor faults with relatively low computational requirements [18]-[19]. The STFT is an extension of the Fourier transform for analyzing nonstationary signals, where the frequency spectrum at different instants of time are analyzed using a narrow sliding time window. More specifically, the analyzed signal $x(t)$ is multiplied by a window function centered at time τ, where a time-localized Fourier transform of the resulting signal is taken for each specific τ [20]. The window function is moved along the time axis and the Fourier transform is performed in each case, yielding a 2-dimensional representation of the signal. The mathematical expression of the STFT is given by

$$STFT(\tau, f) = \int_{-\infty}^{\infty} x(t) \cdot h(t-\tau) \cdot e^{-j2\pi ft} \cdot dt, \qquad (3)$$

where $x(t)$ is the analyzed signal and $h(t)$ is the window function (Hann or Gaussian windows are commonly applied). It can be seen that the $STFT$ (τ, f) is essentially the Fourier transform of $x(t)\cdot h(t-\tau)$. As a result of the STFT, a time domain signal $x(t)$ is decomposed into a 2D time-frequency representation. For the airgap search coil signal, application of STFT provides a 2D time-frequency plot that shows the complete frequency content over the starting transient.

Time-frequency plots of the flux signal of a 4 pole salient pole SM with a healthy rotor and a rotor with broken damper bars during the starting transient can be predicted from Table I, as illustrated in Fig. 4. The frequency contents for a healthy rotor only include the f_s component and rotor saliency components of f_{flux} at integer multiples of k=±$2p$, which are shown in blue solid lines (k=0, ±4, ±8, ±12 shown). When damper bars break in one of the poles, f_{flux} components at integer multiples of k=±1 can also be observed in the time-frequency plot, as shown in red dotted lines in Fig. 4. It should be noted that the "direction" of the f_{flux} components cannot be distinguished with a single search coil, and therefore, the negative frequency components appear as absolute values (Fig. 4). In the time-frequency plot, the x-axis represents "time" during the starting transient, and y-axis represents the "frequency content" of the flux signal, as s decreases from 1 to 0 during rotor acceleration. The main idea of the paper is to determine the presence of broken damper bars by observing the k=±1 components in the STFT plot shown as red dotted lines.

B. 2 Dimensional Finite Element Analysis

A 2 dimensional finite element (FE) analysis was performed with a transient solver on a model of a commercial 6.6 kV, 1 MW, 4 pole salient pole SM shown in Fig. 5(a) to

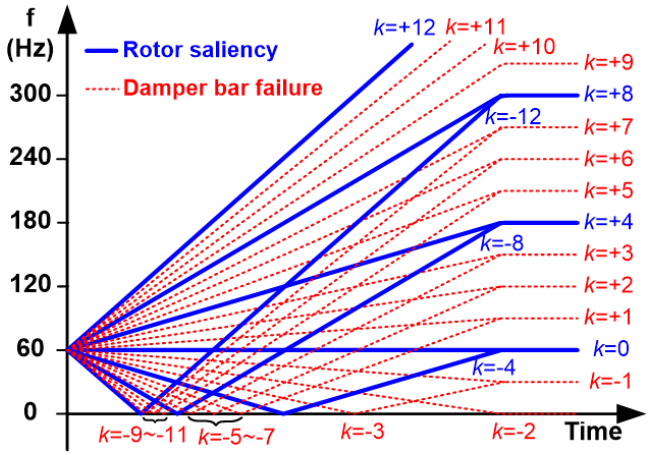

Fig. 4 Time frequency plot: variation in f_{flux} components due to rotor saliency (solid blue lines, k=±$2p$,) and broken damper bars (dotted red lines, k=±1) during 4 pole salient pole SM starting transient ($s: 1 \rightarrow 0$)

verify the claims made on the proposed method for detecting broken damper bars. STFT analysis was performed on the airgap flux data calculated as the motor was started from standstill for cases with and without a broken damper bar at rated voltage. The damper bar on the trailing edge of the pole with the largest current was removed to simulate the fault, as shown in Fig. 5(a), since it is the bar that is most likely to break. A search coil was placed on the tip of the tooth of 1 slot, as shown in Fig. 5(b), for airgap flux measurement. The field winding was short circuited with a starting resistor that has a value 10 times that of the field winding dc resistance.

The STFT time-frequency plots for cases with and without damper bar damage normalized to the f_s component, are shown in Figs 6(a)-(b), respectively. In the STFT plots, the intensity of the lines at any instant of time and frequency at coordinates [x, y] represents the "amplitude" of the frequency component y at the instant of time x. The intensity (or amplitude) of the curves increases with the degree of saliency (multiples of k=±2p) or severity of the damper bar damage (multiples of k=±1 that are not multiples of k=±2p). In Fig. 6(a), the k=±2p (0, ±4, ±8,…) components of f_{flux} produced by rotor saliency can be clearly observed, and are consistent with the predictions made in Table I and Fig. 4. In the STFT plot of the FE analysis with a broken damper bar shown in Fig. 6(b), the increase in the intensity of the components that are integer multiples of k=±1 and not k=±2p can be clearly observed. These broken damper bar induced components (multiples of k=±1) can be seen in between the saliency induced components (multiples of k=±2p), as predicted. Although the 'lines' for the k's are not as clear due to the limited resolution, they are sufficient for determining the presence of broken damper bars. The FE analysis shows that broken damper bar related components (red dotted lines in Fig. 4) produced by the fault can be monitored at the motor starting transient to detect damper bar failures.

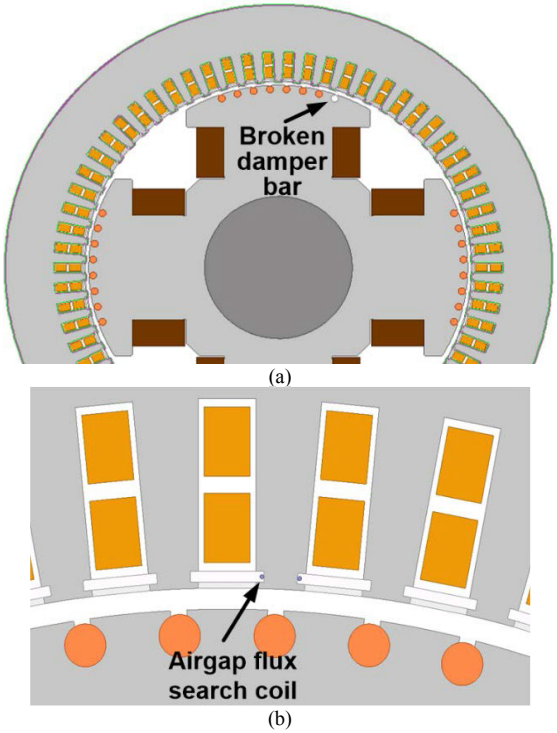

Fig. 5 2 dimensional FE model of a commercial 6.6 kV, 1 MW, 4 pole salient pole SM: location of (a) broken damper bar and (b) airgap flux search coil

IV. Experimental Results

A. Experimental Test Setup

Considering the difficulty in testing medium voltage salient pole synchronous motors in the MW range with broken damper bars, a miniature motor was custom designed and built. The 380 V, 30 kW, 4 pole salient pole SM for verifying the effectiveness of the proposed method under controlled fault conditions, is shown in Fig. 7. The damper and field windings of the rotor with a brushless excitation system were designed to resemble the structure of large salient pole motors. The test rotor included a 144 turn per pole field winding and 6 copper damper bars per pole shorted through 2 sheets of copper lamination on each axial end of the rotor core, as shown in Fig. 7(a). To emulate broken damper bars, 0, 1, and 2 adjacent bars were separated from the end ring copper laminations by cutting the laminations off, as shown in Fig. 7(b). The trailing edge bars of the pole were disconnected since they are most likely to

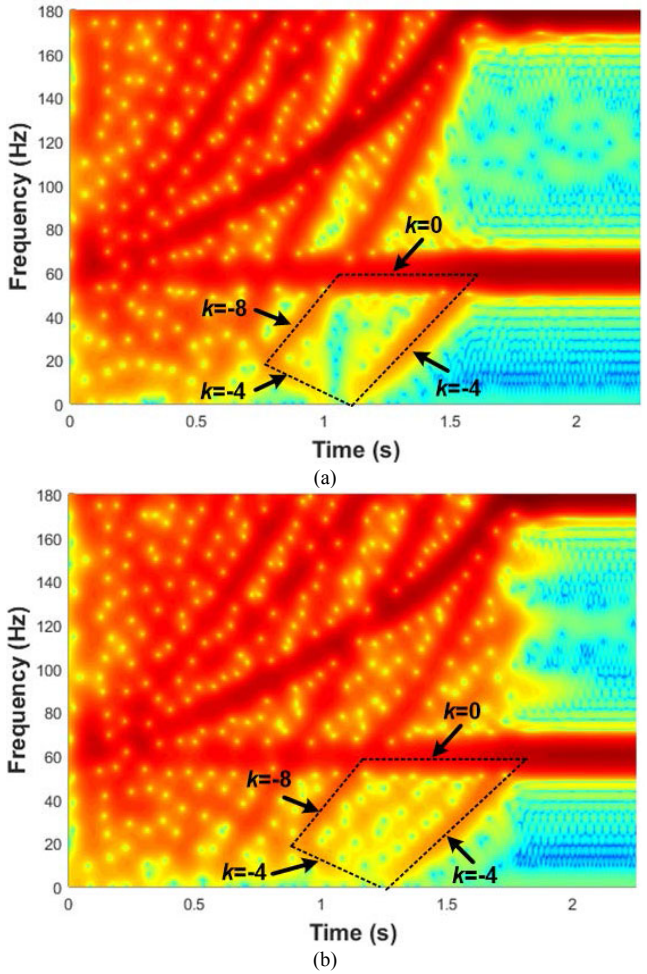

Fig. 6 2 dimensional FE analysis results for commercial 6.6 kV, 1 MW, 4 pole salient pole SM during starting transient: (a) healthy rotor, (b) rotor with 1 broken damper bar

fail in service.

A 10 turn search coil was inserted around one stator tooth to measure the voltage induced by the airgap flux, and the voltage was measured and stored with a commercial data acquisition system. The flux coil voltage measurements obtained with the motor started from the line with 0, 1, 2 broken damper bars were processed off-line. The field winding was short circuited through a starting resistor that has 10 times the value of that of the field winding dc resistance, and the field winding was disconnected from the dc source since only the starting transient data is of interest.

B. Experimental Results

The results of the STFT time-frequency plots of the search coil voltage during the starting transient are shown Fig. 8(a)-(b) for rotors with 0 and 2 broken damper bars, respectively. The frequency range of the STFT plot was set identical to that of Fig. 4 (0-300 Hz) for comparison, and the amplitude was normalized to that of the f_s component. A noticeable change in the pattern of the f_{flux} components in the frequency domain can be clearly observed for the case with 2 broken damper bars. In the STFT plot for the healthy rotor, only the multiples of the k=±4 components of f_{flux} can be observed, as highlighted in Fig. 8(a). The broken damper bar components at integer multiples of k=±1 of f_{flux} appear in the STFT plot of the faulty rotor, as shown in Fig. 8(b). It can be seen that the presence of the saliency and broken damper bar related f_{flux} components are in good agreement with the predictions made in Fig. 4.

A zoomed in view of the search coil voltage STFT time-frequency plots during the starting transient are shown in Fig. 9(a)-(c) for 0, 1, 2 broken damper bars, respectively, for frequency range between 0 and 120 Hz. The existence of the broken damper bar related components (multiples of k=±1 in f_{flux}) and increase in the intensity is evident in Figs. 9(b)-(c). The results clearly demonstrate that the presence and severity of broken damper bars can be detected with high sensitivity during the starting transient with time-frequency analysis of the search coil signals.

V. Conclusion

Airgap search coil based detection of broken damper bars in salient pole synchronous motors was proposed in this paper. The search coil signal is analyzed during the starting transient, when the damper winding is active with maximum current, since it is the most favorable operating condition for detecting damper winding asymmetry. It was shown through an FE analysis and experimental study on a custom-built 30 kW salient pole synchronous motor that broken damper bars can be detected with high sensitivity whenever the motor is started. The proposed method can be implemented without additional hardware for the large synchronous motors equipped with commercial airgap flux coils for field winding turn failure detection purposes. There is currently no known means of detecting damper bars failures for salient pole synchronous machine other than visual inspection, to the best of the authors' knowledge. The proposed method is expected to provide sensitive and reliable detection of damper bar failures and help maintain the reliability and performance of industrial synchronous motors and driven load.

References

[1] G.C. Stone, I. Culbert, E.A. Boulter, H. Dhirani, *Electrical insulation for rotating machines – design, evaluation, aging, testing, and repair*,

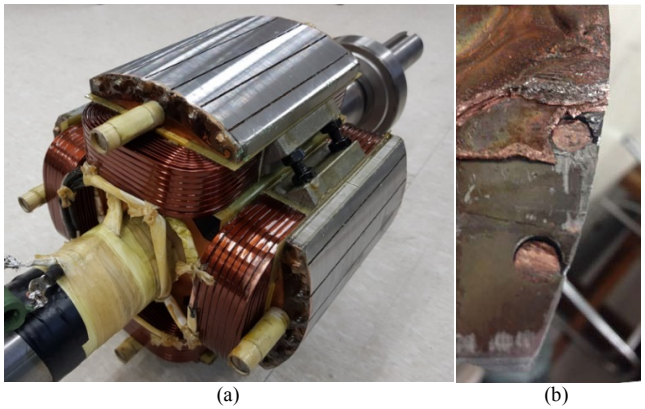

(a) (b)

Fig. 7 Experimental setup - 380 V, 30 kW, 4 pole salient pole synchronous motor; (a) rotor with copper damper bars and field winding; (b) cutting of copper laminations (end ring) for emulation of 0, 1, and 2 broken damper bars

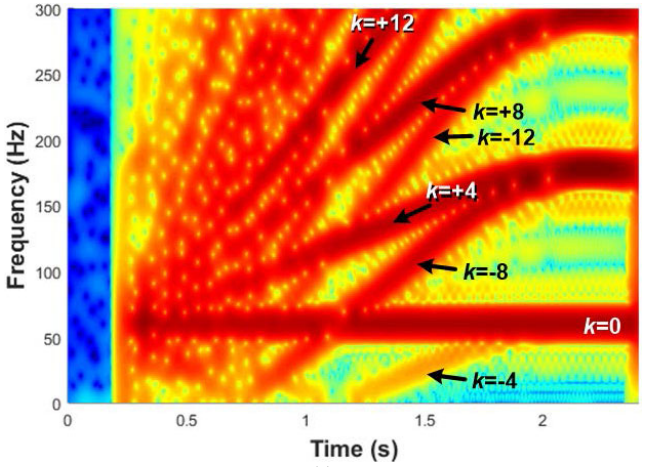

(a)

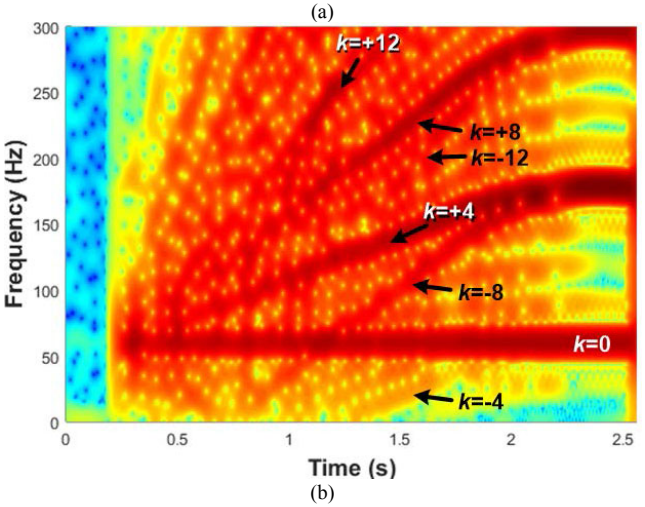

(b)

Fig. 8 STFT time-frequency plots of search coil signal for rotor with (a) 0 and (b) 2 broken damper bars (0-300 Hz)

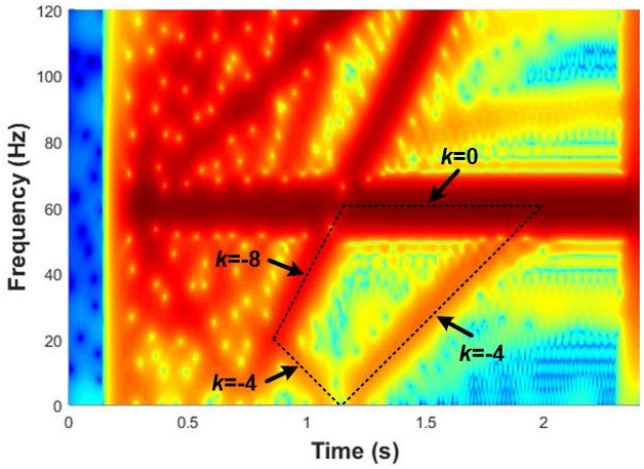

(a)

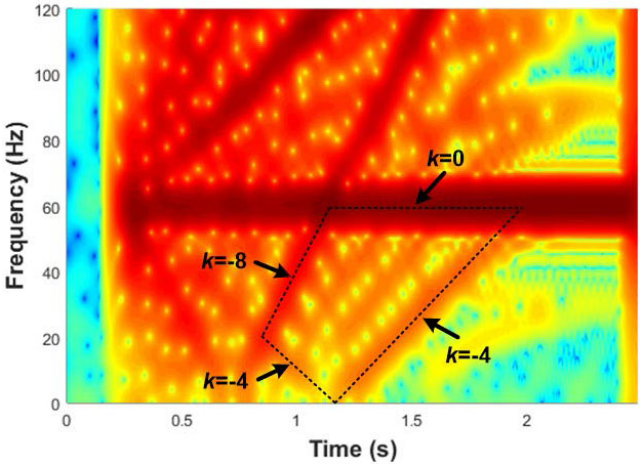

(b)

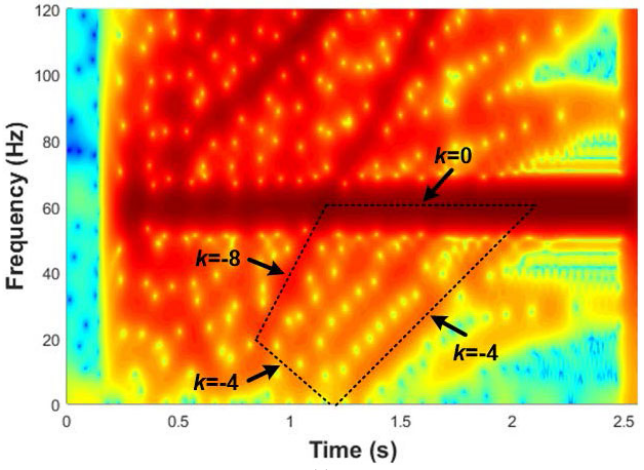

(c)

Fig. 9 Zoomed in view of STFT time-frequency plots of search coil signal for rotor with (a) 0, (b) 1, and (c) 2 broken damper bars (0-120 Hz)

IEEE Press Series on Power Engineering, John Wiley and Sons, 2014.

[2] H.C. Karmaker, "Broken damper bar detection studies using flux probe measurements and time-stepping finite element analysis for salient-pole synchronous machines," *Proc. IEEE SDEMPED*, pp. 193-197, 2003.

[3] P.J. Berry, E.S. Hamdi, "An investigation into damper winding failure in a large synchronous motor," *Proc. of Int'l Univ. Power Eng. Conf.*, pp. 1-4, 2015.

[4] I. Kerszenbaum, *Inspection of large synchronous machines: checklists, failure identification, and troubleshooting*, Wiley-IEEE Press, Apr. 1996.

[5] S.K. Sahoo, P. Rodriguez, M. Sulowicz, "Comparative investigation of fault indicators for synchronous machine failures," *Proc. of ICEM*, pp. 1503-1509, 2014.

[6] P. Rodriguez, "Large SM condition monitoring challenges and pitfalls," *Keynote Address, IEEE SDEMPED*, Aug. 2017.

[7] Alexander Schwery, "Large hydro generators experience and references," *CIGRE Session*, Paris, France 2008.

[8] J. Bacher, "Detection of broken damper bars of a turbo generator by the field winding," *Renewable Energy Power Quality Journal*, vol. 1, no. 2, p. 199-203, Apr. 2004.

[9] J.A. Antonino-Daviu, M. Riera-Guasp, J. Pons-Llinares, J. Roger-Folch, R.B. Pérez, C. Charlton-Pérez, "Toward Condition Monitoring of Damper Windings in Synchronous Motors via EMD Analysis," *IEEE Trans. on Energy Convers.*, vol. 27, no. 2, pp. 432-439, June 2012.

[10] S. B. Jovanovski, "Calculation and Testing of Damper-Winding Current Distribution in a Synchronous Machine with Salient Poles," *IEEE Trans. Power App. and Syst.*, vol. PAS-88, no. 11, pp. 1611-1619, Nov. 1969.

[11] H. Karmaker and Chunting Mi, "Improving the starting performance of large salient-pole synchronous machines," *IEEE Trans. on Magn.*, vol. 40, no. 4, pp. 1920-1928, July 2004.

[12] P. Neti, A. B. Dehkordi, A. M. Gole, "A New Robust Method To Detect Rotor Faults in Salient-Pole Synchronous Machines Using Structural Asymmetries," *Proc. of IEEE IAS Annual Meeting*, pp. 1-8, 2008.

[13] J.E. Berry, "Analysis III: introduction to special vibration diagnostic techniques and how to analysis low, high, and variable speed machines," *Technical Associates of Charlotte*, 1998.

[14] D.R. Albright, "Interturn Short-Circuit Detector for Turbine-Generator Rotor Windings," *IEEE Trans. on Power App. Syst*, vol. PAS-90, no. 2, pp. 478-483, Mar. 1971.

[15] M. Šašić, B. Lloyd and A. Elez, "Finite Element Analysis of Turbine Generator Rotor Winding Shorted Turns," *IEEE Trans. on Energy Convers.*, vol. 27, no. 4, pp. 930-937, Dec. 2012.

[16] M. Sasic, G.C. Stone, J. Stein, C. Stinson, "Detecting Turn Shorts in Rotor Windings: A New Test Using Magnetic Flux Monitoring," *IEEE Ind. Appl. Mag.*, vol. 19, no. 2, pp. 63-69, Mar./Apr. 2013.

[17] G. Oscarson, J. Imbertson, B. Imbertson, S. Moll, "The abc's of synchronous motors," *WEG group*, 2012.

[18] Y. Park, M. Jeong, S. B. Lee, J. A. Antonino-Daviu and M. Teska, "Influence of Blade Pass Frequency Vibrations on MCSA-Based Rotor Fault Detection of Induction Motors," *IEEE Trans. on Ind. Appl.*, vol. 53, no. 3, pp. 2049-2058, May-June 2017.

[19] J. Antonino-Daviu, J. Pons-Llinares, S.B. Lee, "Advanced rotor fault diagnosis for medium-voltage induction motors via continuous transforms," *IEEE Trans. on Ind. Appl.*, vol. 52, no. 5, pp. 4503-4509, Sept./Oct., 2016.

[20] L. Cohen, *Time-Frequency Analysis*. A.V. Oppenheim, Ed. Prentice Hall Signal Processing Series, New Jersey, 1995.